Coherent interaction of an ultrashort zero-area laser pulse with a Morse oscillator

Szczepan Chelkowski and André D. Bandrauk
Département de Chimie, Faculté des Sciences, Université de Sherbrooke, Sherbrooke, Québec, Canada J1K 2R1
(Received 27 December 1989)

Dissociation probabilities, energy absorption, and ground-state populations are calculated numerically for interaction of a Morse oscillator with a resonant ultrashort ($t_p < 10^{-12}$ sec) intense laser pulse as a function of intensity and pulse area in order to investigate the sensitivity of coherence phenomena to delocalization and chaos in molecule-radiation field systems. It is concluded that a zero-area pulse can reduce considerably energy absorbed by a molecule as well as dissociation probabilities for intensities below and near the chaotic region. It is found that the two-level model (describing the interaction of light resonant with the ground to first excited level transition) works well up to the intensity 10^{12} W/cm^2, above which transitions to higher levels must be considered.

I. INTRODUCTION

The resonant interaction of radiation and matter on the time scale shorter than all relevant relaxation times gives rise to coherent effects such as self-induced transparency (SIT) and soliton formation.[1-4] These phenomena are usually described by a model in which matter is represented as an ensemble of two-level systems. If these systems have nondegenerate levels then the Maxwell-Bloch (or Maxwell-Schrödinger) equations reduce to the sine-Gordon equation. This means that electromagnetic radiation pulses can propagate undistorted (as solitons) and without energy loss through a normally absorbing medium. This remarkable effect is modified considerably when the two-level systems are degenerate[5-7] since then the resulting propagation equation is not integrable (except in some particular cases[5-7]) and thus one does not know whether distortionless pulses can be formed. However, it follows from the propagation equation integrated over time, see, e.g., equation (8) from Ref. 5, that in this case pulse absorption will be greatly reduced for certain values of the pulse area S defined by the formula

$$S=(p/\hbar)\int_{-\infty}^{\infty}\epsilon(t,z)dt\ , \tag{1}$$

where p is the transition dipole moment and $\epsilon(t,z)$ is the slowly varying electron-field envelope. The complete vanishing of absorption in this degenerate case occurs for a pulse having the area S equal to zero. An example of this is a pulse consisting of two pulses whose phase differs by π. Such a pulse may eventually spread in the the degenerate case (in the nondegenerate case a pulsating soliton can be formed[2]) and will not be absorbed until its width approaches the dephasing time T_2. Recently, we showed[8,9] that a similar situation occurs when light propagates in a medium consisting of systems having N-equidistant levels. Such a model is certainly more adequate than two-level models for the description of the propagation of radiation resonant with molecular vibrations or rotations,[10] in particular, when the Rabi frequencies approach the detuning present in molecular systems.[8-10] We showed that the coupled Maxwell-Schrödinger equations describing the propagation of ultrashort pulses reduce then to a *multisine-Gordon equation* which predicts that zero-area pulses are not absorbed and the absorption depends strongly on the pulse area, having deep minima for certain values of the area.[8]

In this paper we investigate a model in which an ionic molecule represented as a Morse oscillator interacts with a zero-area laser pulse. The radiation is taken to be resonant with the transition from the fundamental to the first excited vibrational level. Thus this model is more realistic then the above-mentioned N-equidistant level model since it includes the detuning resulting from the anharmonicity of the molecular potential and also transitions to continuum states but requires a full numerical treatment. In our previous models the transition amplitudes and the laser induced medium polarization were found analytically from the Schrödinger equation as functions of pulse area.[8] In this paper we present the results of a numerical integration of the time-dependent Schrödinger equation allowing us to investigate the response of a Morse oscillator to a zero-area pulse and thus to see how the above-mentioned coherent effects are modified in the presence of important multiphoton transitions to higher vibrational levels as well as to the continuum states (dissociation of the molecule). Recently, there appeared in the literature a number of papers in which strong radiation interaction with atoms or molecules is treated nonperturbatively by solving numerically the time-dependent Schrödinger equation.[11-16] Most of these are devoted to the above-threshold ionization phenomenon (ATI). The interaction of a Morse oscillator with an intense continuous radiation was already discussed in Refs. 11-13. In particular, Ref. 11 discusses the importance of chaos in multiphoton excitation of molecules. This problem had been discussed earlier in a number of papers,[17] in which the molecule was represented as an anharmonic oscillator.

II. MODEL CALCULATIONS

Our model is based on the Schrödinger equation with the Hamiltonian

$$H=\frac{-\hbar^2}{2m}\frac{\partial^2}{\partial x^2}+D[1-\exp(-ax)]^2 - d_1 x E_M U(t)\cos(\omega_L t)\ , \tag{2}$$

where $x=r-r_0$, r_0 is the equilibrium separation of nuclei, d_1 is the effective charge or dipole gradient, E_M is the maximum value of the radiation electric field, and $U(t)$ is the pulse envelope chosen to equal 1 at the maximal value of the electric field. The energy eigenvalues E_n and normalized eigenfunctions ψ_n of the Morse oscillator are[11,12,18]

$$E_n=BD(n+\tfrac{1}{2})[2-B(n+\tfrac{1}{2})]\ , \tag{3}$$

$$\psi_n=C_n y^s \exp(-y/2)M(-n,2s+1,y)\ , \tag{4}$$

where

$$B=\left[\frac{\hbar a^2}{2mD}\right]^{1/2},\quad y=\frac{2}{B}\exp(-ax),\quad s=1/B-n-\tfrac{1}{2}\ , \tag{5}$$

$$C_n=\left[\frac{a\Gamma(2/B-n)2s}{n!\Gamma(2/B-2n)^2}\right]^{1/2}, \tag{6}$$

and $M(-n,2s+1,y)$ is the confluent hypergeometric function (Kummer's function) being equal, in the case of integer n (up to a multiplicative factor) to the generalized Laguerre polynomial[19] $n=0,1,\ldots,n<1/B-\frac{1}{2}$. Using the same dimensionless variables as in Ref. 11 we rewrite the Schrödinger equation in the form

$$i\frac{\partial\psi}{\partial\tau}=\left[-\frac{\partial^2}{\partial X^2}+B^{-2}[1-\exp(-X)]^2 - KXU(t)\cos(\mu\tau)\right]\psi\ , \tag{7}$$

where

$$\tau=DB^2t/\hbar,\quad X=ax,\quad K=d_1E_M/aDB^2\ , \tag{8}$$

$$\mu=\hbar\omega_L/DB^2\ . \tag{9}$$

We have integrated numerically Eq. (7) for various values of the peak laser intensity $I=(c/8\pi)E_M^2$ (the light is assumed to be linearly polarized) using the following values of parameters present in (5)–(9): $B=0.0419$, $D=6.125$ eV, $a=1.1741a_0^{-1}$, $d_1=0.786Db/a_0$, $r_0=1.7329a_0$. These numbers correspond to the HF molecule and were taken from Refs. 11 and 12. For these parameters the Morse potential supports 24 bound states and its characteristic vibrational time is $t_c=\hbar/[E(1)-E(0)]=8.41\times10^{-15}$ sec which is equal to the light cycle because of our choice of light frequency ω_L resonant with the transition from the ground state to the first excited level. The pulse envelope function was chosen either as

$$U(t)=|\sin(\pi t/t_p)|\ , \tag{10a}$$

or as

$$U(t)=\sin(\pi t/t_p)\ , \tag{10b}$$

where $0<t<2t_p$. The first envelope (10a) describes a sequence of two equal phase pulses each of duration t_p while (10b) describes a corresponding *zero area pulse,* since the second pulse is now out of phase by π.

The time evolution of the wave function described by (7) was carried out according to an implicit Crank-Nicholson scheme

$$\left[1+\frac{i\delta\tau}{2}H_1(\tau+\delta\tau/2)\right]\psi(\tau+\delta\tau) = \left[1-\frac{i\delta\tau}{2}H_1(\tau+\delta\tau/2)\right]\psi(\tau)\ , \tag{11}$$

where H_1 is the dimensionless Hamiltonian defined by the right-hand side of Eq. (7). After discretizing the X variable and approximating the space derivative in point X_m by the formulas

$$\frac{\partial^2\psi}{\partial X^2}=\frac{\psi_{k+1}-2\psi_k+\psi_{k-1}}{\delta X^2},\quad \psi_k=\psi(X_k,t)\ ,$$
$$X_k=-ar_0/2+k\delta X \tag{12}$$
$$k=0,1,\ldots,k_M,\quad \psi_0=\psi_{k_M}=0$$
for any t (boundary condition),

Eq. (11) reduces to a tridiagonal system of linear equations which is solved using the algorithm given in Ref. 20. More details concerning this integration scheme can be found in Refs. 16 and 20 (because of the very steep increase of the potential for r approaching zero it was sufficient to start our X grid at $X=-ar_0/2$ instead of $X=-ar_0$). In the calculations reported below the time and space steps and k_M vary as a function of the laser intensity and total pulse duration, the extreme case being $\delta t=\delta\tau\hbar/DB^2=0.037\hbar/D=0.0005$ cycle, 1 cycle $=t_c=8.41\times10^{-15}$ sec, $\delta x=0.0085a_0$, $k_M=5000$. The last number means that we confined our oscillator in a box of size about $44a_0$. The final choice of values of these parameters was done after having performed numerous test runs yielding negligible sensitivity of the results to values of δt, δx, and k_M.

Having found the wave function we calculated the dissociation probability $P_D(t)$, energy absorbed $A(t)$ and the population of the ground state $P_0(t)$ using the formulas

$$P_D(t)=1-\sum_{n=0}^{23}|\langle\psi_n|\psi(t)\rangle|^2\ , \tag{13}$$

$$A(t)=(\langle\psi|H_{\rm mol}|\psi\rangle-E_0)/D\ , \tag{14}$$

$$P_0(t)=|\langle\psi_0|\psi\rangle|^2\ , \tag{15}$$

where $H_{\rm mol}$ is the Hamiltonian of a free molecule. We display in Figs. 1–3 these quantities calculated for the time $t=2t_p$ (i.e., at the time when the second pulse is switched off) as functions of peak pulse intensity. Since the coherent resonant effects are expected to depend on the pulse area[8] we display each quantity in two different ways; we either varied the peak intensities keeping the area S [this is an area of one pulse of the pulse sequence described by formula (10)] fixed [Figs. 1(a), 1(b), 2(a), 2(b),

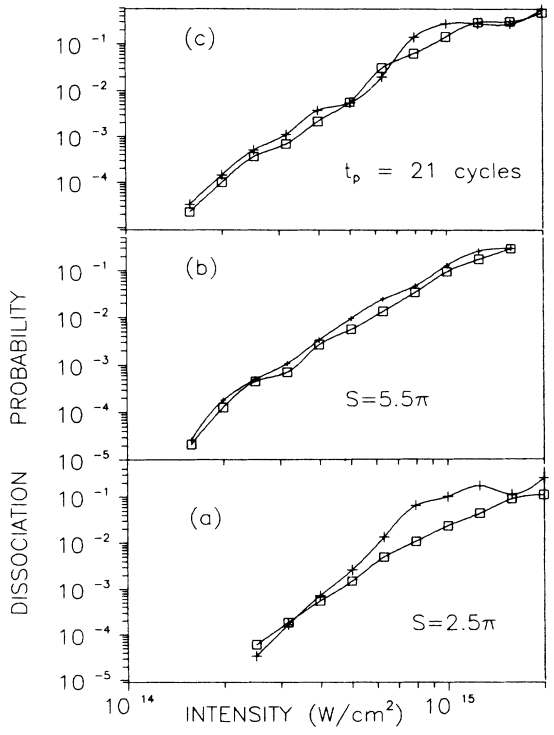

FIG. 1. Dissociation probability P_D at $t=2t_p$ as a function of pulse peak intensity I at fixed (a) area $S=2.5\pi$; (b) area $S=5.5\pi$; (c) individual pulse duration $t_p=21$ cycles (1 cycle $=8.41\times10^{-15}$ sec). The parameters t_p, S, and I are related by (17). □, zero-area pulse sequence described by Eq. (10b); +, nonzero-area sequence described by Eq. (10a). The abscissa on the right displays values of molecular energy expectation values.

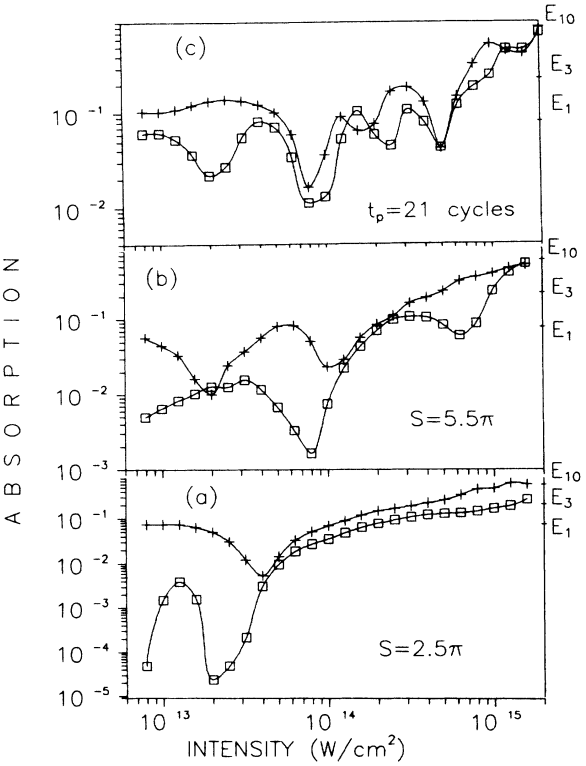

FIG. 2. Absorption A defined by formula (14) as a function of peak intensity I. □, zero-area pulse sequence described by Eq. (10b); +, nonzero-area sequence described by Eq. (10a) (same parameters as in Fig. 1).

3(a), and 3(b)] or varied the intensity keeping the pulse duration t_p fixed [Figs. 1(c), 2(c), and 3(c)]. The pulse area S was calculated using the transition dipole moment p calculated with the help of the expression

$$p=p_{01}=d_1\langle\psi_1|x|\psi_0\rangle=d_1(B/2)^{1/2}/a=0.097Db \ . \quad (16)$$

The relation between the individual pulse area S, intensity I, and pulse duration t_p can be found from the following formulas:

$$S=p_{01}E_M/\hbar\int_0^{t_p}U(t)dt, \quad t_p(c)=2.215\times10^7 S/I^{1/2} \ . \quad (17)$$

In the last formula the intensity is expressed in W/cm^2 and time in cycles. The total area of the pulse sequences described by (10) was either $2S$ (lines with crosses) or zero (lines with squares). One concludes from Fig. 1 that for $S=2.5\pi$ the zero-area pulse leads to a decrease of dissociation compared to the nonzero-area sequence by a factor approaching 10; for an area $S=5.5\pi$ this factor never exceeds 2. The difference between a zero-area and nonzero-area pulse sequence is much sharper for the absorption $A(2t_p)$ and the ground-state population $P_0(2t_p)$ as shown in Figs. 2 and 3. Also the sensitivity on the

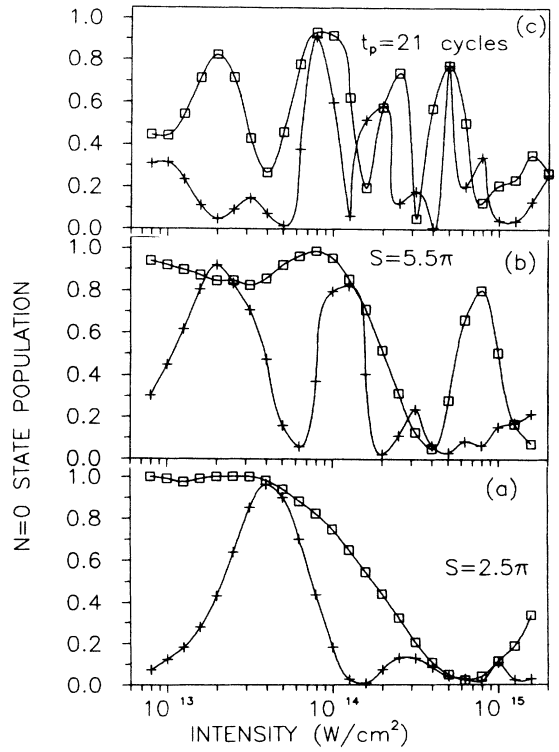

FIG. 3. Ground-state population defined by (14) as a function of pulse peak intensity I. □, zero-area pulse sequence described by Eq. (10b); +, nonzero-area sequence described by Eq. (10a) (same parameters as in Fig. 1).

pulse area magnitude is much stronger here; this explains the rapid variation of the absorption and ground-state population observed in Figs. 4(b) and 4(c), since this is the case when the pulse duration is fixed and the area changes from 0.85π to 13.5π. Finally, Fig. 4 shows the dissociation, absorption, and ground-state population as functions of time for intensity $I=7.9\times10^{14}$ W/cm^2 and $S=2.5\pi$.

III. RESULTS AND DISCUSSION

The present work was motivated by the results of our earlier investigation[8,9] showing that a zero-area pulse interacting with a molecule modeled by N-equidistant levels should not be absorbed at all (for durations shorter than any medium relaxation or dephasing time) and that its absorption as a function of pulse area should exhibit deep minima for certain values of the pulse areas. For this reason we chose to investigate here two successive pulse sequences of individual area S equal to 2.5π (5.5π) such that the total area of each sequence would be either 5π (11π) or zero. In a two-level system, the first pulse sequences (with nonzero area) would lead to the complete inversion of the system, whereas the zero-area sequence would return the system completely to the initial state. We first conclude that the two-level model works very well up to the intensity $I_T=10^{12}$ W/cm^2, i.e., we found

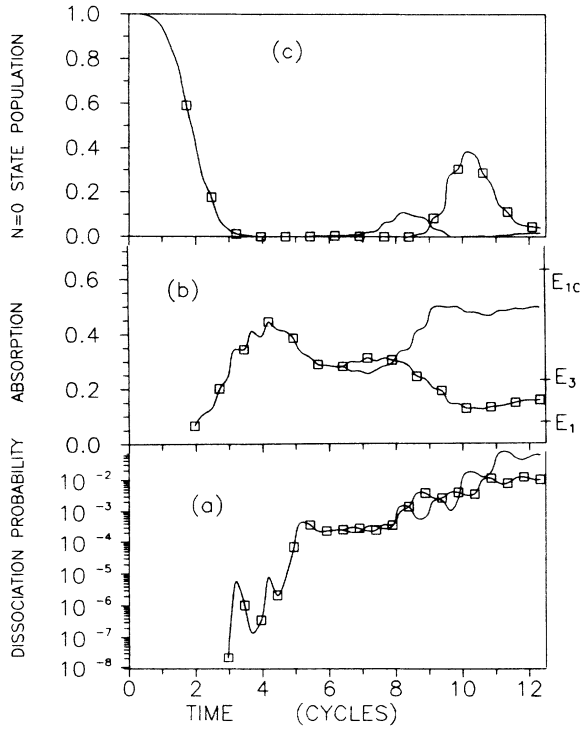

FIG. 4. Time dependence of (a) dissociation probability $P_D(t)$, (b) absorption $A(t)$, and (c) ground-state population $P_0(t)$ calculated for peak intensity $I=7.9\times10^{14}$ ($S=2.5\pi$). □, zero-area pulse sequence described by Eq. (10b); ——, nonzero-area sequence described by Eq. (10a). The abscissa on the right in (b) displays molecular energy expectation values.

that the ground-state population and absorption calculated with our algorithm coincide with the two-level model predictions, the dissociation probability P_D being smaller than the accuracy limits of our programs (i.e., $P_D<10^{-9}$ for I close to I_T). Such a high value of I_T can be easily attributed to the fact that the anharmonicity of the HF molecule is very large leading to a detuning Δ of the transition from the first to the second excited level. One easily finds using Eq. (3) that $\Delta=2B^2D=173.46$ cm^{-1}. According to arguments given in Refs. 9 and 10, virtual transitions to the second excited level will occur if the corresponding Rabi frequency $\Omega_R=p_{12}E_M/\hbar=6.32\times10^{-5}I^{1/2}$, where I is W/cm^2 and Ω_R in cm^{-1}, becomes comparable to the detuning Δ. This occurs when the laser intensity is close to 10^{13} W/cm^2, for which $\Omega_R\cong200$ cm^{-1}. Thus the delocalization of the molecular wave function $\psi(x,t)$ is inhibited by the detuning below 10^{13} W/cm^2. This fact explains also the relatively low dissociation probabilities shown in Fig. 1. We expect that both the wave-function delocalization and the dissociation probability will be greater for molecules having smaller values of this detuning Δ. In order to illustrate better the wave-function delocalization we add a right-hand side axis in Figs. 2 and 4(b) for the molecular energy expectation values $\langle\psi|H_{\rm mol}|\psi\rangle$. One observes a considerable delocalization of the wave function at time $t=2t_p$ above $I=10^{14}$ W/cm^2 (i.e., the expectation value of the energy exceeds the energy of the first excited level E_1 in this intensity region). The time plot of the molecular energy, Fig. 4(b), shows that even at intensities as high as $I=7.9\times10^{14}$ the zero-area pulse reverses delocalization in the second time interval $t_p<t<2t_p$. In other words, at this intensity the coherence is still clearly visible. These coherent effects become visibly smaller in all our figures, at intensities above 10^{15} W/cm^2 for which, according to the results of Ref. 11, one approaches the regime in which the Morse oscillator exhibits *chaotic* behavior. In the calculations presented here we took values of parameters corresponding to the HF molecule because we wanted to compare our results with the study of chaotic behavior in HF presented in Ref. 11, even though one should not forget that in this regime of intensities ($I>10^{15}$ W/cm^2) one should consider ionization of atoms (rates of 10^{12} s^{-1}, at $I=10^{14}$ W/cm^2, are predicted, see Refs. 21 and 22). This means that for such high intensities one approaches the limit of the applicability of the model based on Hamiltonian (2). However, the phenomena discussed here will occur at lower intensities in molecules having lower anharmonicities, i.e., according to our estimate concerning Rabi frequencies Ω_R presented above, we expect the changing a molecule should roughly lead to the rescaling of the intensity axis by $(\alpha/\alpha_{\rm HF})^2$, where $\alpha=\Delta/P_{01}$ ($\alpha_{\rm HF}=\alpha$ for HF) and Δ,p_{01} are the anharmonicity and transition dipole moment of another molecule. Thus we expect that for molecules having smaller α the chaotic region will be shifted towards lower intensities.

Of note is that the dissociation probability is less sensitive to coherent effects than the absorption and ground state population, the last one being clearly most affected by them. Thus Figs. 2(b) and 2(c) show that the zero-area

pulse sequence leads to a dissociation about half that of a nonzero-area sequence. We think that this is related to the fact, that a significant part of the dissociation is occuring via a tunneling mechanism[22,23] which is completely insensitive to the pulse phase history. Thus the second part of the zero-area pulse, as seen in Fig. 4, by tending to populate only lower levels, lowers the dissociation rates, but the dissociation caused by the first part cannot be reversed in the framework of this tunneling scheme. Obviously, one sees that this tunneling mechanism is not always dominant here; the dissociation probability shown in Fig. 4(b) shows oscillatory behavior related to the resonant, coherent character of processes investigated here, while the tunneling mechanism leads to monotonically increasing dissociation probabilities[22,23] (as a function of time).

Finally, we interpret the maxima of the ground-state populations in Fig. 3(c) which correlate with minima in the corresponding absorption plot [Fig. 2(c)]. These occur for both pulse sequences at intensities 8×10^{13}, 2×10^{14} (2.5×10^{14} W/cm^2, for a zero-area sequence) and 5×10^{14} corresponding to individual pulse area $S=8.4$, 13.4 (15, for a zero-area sequence), and 21.2 (two of them occur at same values of S for both pulse sequences). These values are close to the areas for which absorption minima occur in a three-level harmonic system. One finds, using formula (45) of Ref. 9 that such a three-level system returns completely to the ground state for areas $S=2\pi n/\lambda_1=7.25\times n$, where $\lambda_1=0.5[1+(p_{12}/p_{01})^2]^{1/2}$ and $n=0,1,2,\ldots$. Note that the zero-area pulse shown in Fig. 3(c) does not return the system completely to the ground state already at intensities around 10^{13} W/cm^2. This is related to the fact that the pulse is very short ($t_p=21$ cycles) and thus its spectral width is close to the detuning Δ. The plots shown in Figs. 3(a) and 3(b) describe longer pulses in this intensity region and lead to populations of the ground state close to 1 for zero-area pulses up to the intensity 10^{14} W/cm^2. We have verified that for much longer pulses ($t_p=100$ cycles) this limiting intensity is even closer to 10^{15} W/cm^2, the chaotic regime border. However, even for a short pulse the difference between the two pulse sequences is clearly visible in the time dependence of the population plotted in Fig. 4(c).

Summarizing, we note that our study shows that there exist pulses which minimize the energy absorbed by a Morse oscillator. It remains to be investigated how stable are such pulses, i.e., can they exhibit SIT when propagating in a medium consisting of Morse oscillators. We are currently pursuing this question.

ACKNOWLEDGMENTS

We wish to thank the Natural Sciences and Engineering Research Council of Canada for special grants to investigate these problems.

[1] J. Allen and J. H. Eberly, *Optical Resonance and Two-Level Atoms* (Wiley, New York, 1975).
[2] G. L. Lamb, Jr., Rev. Mod. Phys. **43**, 99 (1971).
[3] G. L. Lamb, Jr., *Elements of Soliton Theory* (Wiley, New York, 1980).
[4] M. E. Crenshaw and C. D. Cantrell, Phys. Rev. A **37**, 3338 (1988); Opt. Lett. **13**, 386 (1988).
[5] C. K. Rhodes, A. Szöke, and A. Javan, Phys. Rev. Lett. **21**, 1151 (1968).
[6] R. K. Dodd, R. K. Bullough, and S. Duckworth, J. Phys. A **8**, L64 (1975).
[7] S. Duckworth, R. K. Bullough, P. J. Caudrey, and J. D. Gibbon, Phys. Lett. A **57**, 19 (1976).
[8] S. Chelkowski and A. D. Bandrauk, in *Atomic and Molecular Processes with Intense Laser Pulses,* Vol. 171 of *NATO Advanced Study Institute, Series B: Physics,* edited by A. D. Bandrauk (Plenum, New York, 1988), p. 57.
[9] S. Chelkowski and A. D. Bandrauk, J. Chem. Phys. **89**, 3618 (1988).
[10] C. D. Cantrell, V. S. Letokhov, and A. A. Makarov, in *Coherent Nonlinear Optics Recent Advances,* edited by M. S. Feld and V. S. Letokhov (Springer-Verlag, Berlin, 1980), p. 187.
[11] M. E. Goggin and P. W. Milonni, Phys. Rev. A **37**, 796 (1988).
[12] R. B. Walker and R. K. Preston, J. Chem. Phys. **67**, 2017 (1977).
[13] R. Heather and H. Metiu, J. Chem. Phys. **86**, 5009 (1987).
[14] C. Cerjan and R. Kosloff, J. Phys. B **20**, 4441 (1981).
[15] M. D. Perry, A. Szöke, and K. C. Kulander, Phys. Rev. Lett. **63**, 1058 (1989) and references therein.
[16] J. Javanainen, J. H. Eberly, and Qichang Su, Phys. Rev. A **38**, 3430 (1988).
[17] J. R. Ackerhalt and P. W. Milonni, Phys. Rev. A **34**, 1211 (1986); **34**, 5137 (1986); P. W. Milonni, J. R. Ackerhalt, and M. E. Goggin, Phys. Rev. A **35**, 1714 (1987).
[18] F. V. Bunkin and I. I. Tugov, Phys. Rev. A **8**, 601 (1973).
[19] *Handbook of Mathematical Functions,* edited by M. A. Abramowitz and I. A. Stegun (Dover, New York, 1965).
[20] W. H. Press, B. P. Flannery, S. A. Teukolsky, and W. T. Vettering, *Numerical Recipes* (Cambridge University Press, Cambridge, 1986), p. 40.
[21] S. L. Chin, C. Rolland, P. B. Corkum, and P. Kelly, Phys. Rev. Lett. **61**, 153 (1988).
[22] N. H. Burnett and P. Corkum, J. Opt. Soc. Am. **6**, 1195 (1989).
[23] L. V. Keldysh, Zh. Eksp. Teor. Fiz. **47**, 1945 (1964) [Sov. Phys.—JETP **20**, 1307 (1965)].